Steel and Composite Structures, *Vol. 26, No. 6* (*2018*) *705-717*
DOI: https://doi.org/10.12989/scs.2018.26.6.705

Numerical study on axially loaded ultra-high strength concrete-filled dual steel columns

David Pons, Ana Espinós *, Vicente Albero and Manuel L. Romero

Instituto de Ciencia y Tecnología del Hormigón (ICITECH), Universitat Politècnica de València, Valencia, Spain

(*Received October 3, 2017, Revised December 15, 2017, Accepted January 12, 2018*)

Abstract. This paper presents a numerical investigation on the mechanical performance of concrete-filled dual steel tubular columns of circular section subjected to concentric axial load. A three-dimensional numerical model is developed and validated against a series of experimental tests. A good agreement is obtained between the experimental and numerical results, both in the peak load value and in the ascending and descending branches of the load-displacement curves. By means of the numerical model, a parametric study is carried out to investigate the influence of the main parameters that determine the axial capacity of double-tube columns, such as the member slenderness, inner and outer steel tube thicknesses and the concrete grade – of both the outer concrete ring and inner core –, including ultra-high strength concrete. A total number of 163 numerical simulations are carried out, by combining the different parameters. Specific indexes are defined (Strength Index, Concrete-Steel Contribution Ratio, Inner Concrete Contribution Ratio) to help rating the relative mechanical performance of dual steel tubular columns as compared to conventional concrete-filled steel tubular columns, and practical design recommendations are subsequently given.

Keywords: finite element model; concrete-filled dual steel tubular columns; ultra-high strength concrete; slender columns

1. Introduction

Concrete-filled dual steel tubular (CFDST) columns are a structural solution of recent development, consisting of two concentric steel tubes with a concrete infill. The concrete infill may be only present at the ring between the two steel tubes – double-skin solution (Fig. 1(a)) – or also filling the inner tube – double-tube solution (Fig. 1(b)) –. The interest in developing lighter composite columns is growing in the field of infrastructures, since the self-weight reduction of vertical members provides an enhanced response to seismic loads (Han *et al*. 2014). According to Elchalakani *et al*. (2002), apart from the own benefits of traditional concrete-filled steel tubular (CFST) columns, double-tube columns possess other additional benefits that make them interesting for high-rise buildings, such as: higher ductility, higher energy absorption and, most importantly, improved fire resistance due to the thermally protected inner tube (Tao *et al*. 2004, Romero *et al*. 2015).

Parallel to this, the use of high-strength concrete (HSC) has become more frequent, owing to the improvements in its production technology and the reduction of the manufacturing costs. In this sense, ultra-high strength concrete (UHSC) is being used in slender structural members given their important advantages, mainly in members subjected to high compressive loads, as it occurs in columns within high-rise buildings and bridge piers. The simultaneous use of UHSC in double-tube columns creates

(a) Double-skin section

(b) Double-tube section

Fig. 1 Different types of sections in CFDST columns

*Corresponding author, Ph.D.,
E-mail: aespinos@mes.upv.es

ISSN: 1229-9367 (Print), 1598-6233 (Online)

an ideal synergy, allowing for more slender members with reduced cross-sections.

Nevertheless, at present, designers feel unwilling to use this solution for several reasons. Firstly, the current guidance in the reference standards do not provide updated analytical expressions or design recommendations for this type of columns, due to the fast evolution of composite construction. Furthermore, Eurocode 4 Part 1-1 (CEN 2004b) limits the concrete strength to 50 MPa for the calculation of the column capacity. Apart from that, the brittle nature of high strength concrete and the premature failure of slender members under certain loading conditions make necessary to study new solutions that guarantee a suitable structural response.

The wide number of investigations carried out in stub double-skin columns, summarized by Zhao and Han (2006), agree in that the compressive behaviour of such columns may be explained with the outer steel tube and the concrete ring working together as in a CFST column, where the steel tube confines the inner concrete, increasing its compressive strength. At the same time, the inner steel tube is considered working isolated as a hollow tube.

Up to now, limited experimental work has been carried out on slender double-tube columns filled with normal strength concrete (NSC). From the scarce literature, it is worth mentioning the work from Chen *et al.* (2015) using slender double-tube columns with polygonal section which failed by overall buckling. Other authors such as Essopjee and Dundu (2015) found the same type of failure due to global instability in slender columns.

Previous experimental campaigns were carried out by the authors of this paper, where the load-bearing capacity at room temperature of 14 slender circular CFDST columns under axial load was analysed (Romero *et al*. 2017), following by other 12 tests on CFDST columns subjected to eccentric load (Ibañez *et al*. 2017). The effect of UHSC on the mechanical response of CFDST columns was investigated in this research. It was found that the use of UHSC as concrete infill on CFDST is not worthy since second order effects in slender columns neglect any possible improvement of the bearing capacity.

Also the fire resistance of CFDST columns was previously investigated by the authors (Romero *et al*. 2015), through a series of six fire tests on double-tube concrete filled steel tubular slender columns with different combinations of concrete strength. The main conclusion obtained from this experimental investigation was that a good design strategy for composite columns is to split thick CHS tubes in two different steel tubes with the same total steel area, but placing the thinner CHS in the outer part of the section and the thicker CHS in the inner part, so as to be thermally protected.

In the present paper, the mechanical behaviour of CFDST columns is numerically studied through a three-dimensional finite element model. The adopted values of the parameters of the model are the result of an extensive sensitivity analysis. The accuracy of the numerical model is assessed by comparison with experimental tests and, once a validated numerical model is available, a comprehensive parametric study is carried out with the aim of evaluating the influence of the main factors that affect the load-bearing capacity of CFDST columns and providing practical design recommendations.

This numerical study focuses on slender CFDST columns with circular section, totally or partially infilled with concrete – i.e. double-tube or double-skin –, using NSC, HSC or UHSC and subjected to concentric axial load, in order to reach more understanding on the mechanical behaviour of these columns and the influence of the type of concrete filling on their bearing capacity. It is aimed to investigate what are the situations where the use of HSC or UHSC is appropriate and where is more efficient to place it – at the inner core, outer ring or at both –. The aim of this study is to provide designers with practical recommendations on the use of this type of composite columns in construction and the convenience of using high performance concrete.

2. Description of the numerical model

2.1 General

The nonlinear finite element package Abaqus (ABAQUS 2014) was used for modelling the mechanical response of slender CFDST columns, in order to develop a realistic three-dimensional numerical model that predicts with accuracy the behaviour of this type of columns. The authors have long time experience in numerical modelling of CFT columns using Abaqus, in fact this numerical model for CFDST columns is an evolution of previous models (Espinos *et al*. 2010). The main parameters of the model were the uniaxial stress-strain relations of the materials (obtained by means of experimental coupon tests), the mesh size and the interactions between the contacting surfaces, which values were previously obtained through a sensitivity analysis (Pons Aliaga 2016).

2.2 Geometry and boundary conditions

In order to reduce the computational cost of the numerical simulations, only a quarter of the column was modelled (Figs. 2(a)-(b)). The model consisted of the following parts: concrete core, concrete ring, outer and inner steel tube, steel end plate and knife-edge bearing.

The steel end plate and the knife-edge bearing were considered perfectly elastic bodies, allowing for the load introduction, which was uniformly transferred to the rest of the column components by means of an imposed displacement. The column ends were assumed hinged and modelled through a pinned end at the knife-edge bearing.

2.3 Finite element mesh

All the parts of the model, except for the knife-edge bearing, were meshed with eight noded three-dimensional solid elements (C3D8R). In turn, the knife-edge bearing was meshed with thetraedral solid elements (C3D10). The mesh density was controlled based on the results of a mesh sensitivity study, obtaining an optimal FE size of 20 mm (Fig. 3).

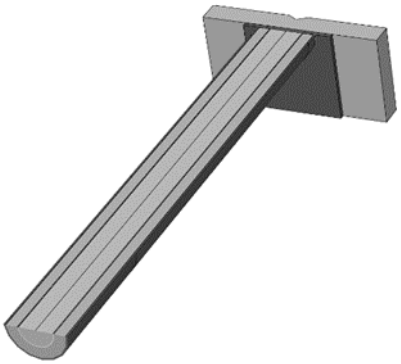

(a) Geometry of the model

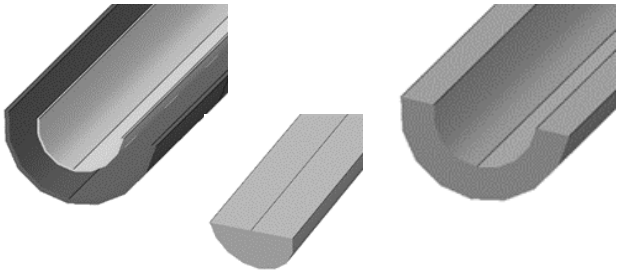

(b) Parts of the model: Outer and inner steel tube, concrete ring and concrete core

Fig. 2 Three-dimensional numerical model of a CFDST column

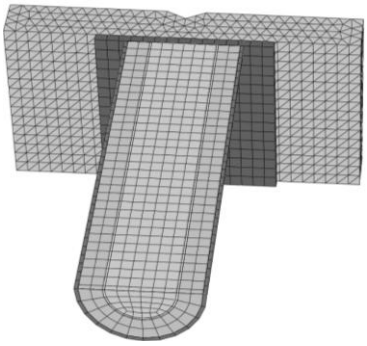

Fig. 3 Finite element mesh of the model

2.4 Materials

The materials used in the numerical model were considered continous, homogeneous and isotropic. Elastic-plastic models were defined, using measured values obtained from the material tests, together with the appropriate yield criterion, accounting for the triaxial stress state of concrete and the biaxial behaviour of the steel tube. Both the steel end plate and the knife-edge bearing were defined as elastic parts, for which the nominal values were obtained from Eurocode 3 Part 1.1 (CEN 2015): elastic modulus (E = 210 GPa) and Poisson's ratio (v = 0.3).

2.4.1 Steel

According to the results of a previous sensitivity analysis (Pons Aliaga 2016), the most accurate constitutive model for the cold-formed hollow steel tubes was that of

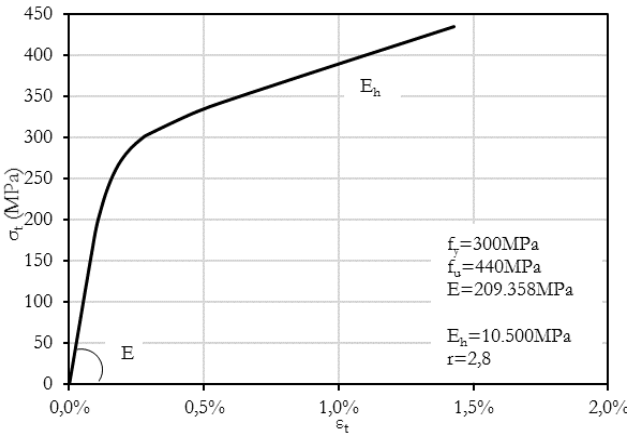

Fig. 4 Uniaxial model by Menegotto-Pinto

Menegotto and Pinto (1973), given its gradual transition from a linear elastic curve to a post-yield hardening branch.

The complete definition of this model may be established by means of five parameters: elastic modulus (E), yield strength (f_y), ultimate strength (f_u), the hardening modulus of yielded steel (E_h) and the index r, which has effects on the curvature of the diagram. Fig. 4 shows the stress-strain curve proposed by Menegotto and Pinto (1973), which was adjusted by Portoles *et al*. (2011b) for slender hollow circular columns and experimentally limited to f_u.

The equation of Menegotto-Pinto constitutive model for steel, limited to f_u is as follows

$$\frac{\sigma}{f_y} = bX + (1-b)\frac{X}{(1-|X|^r)^{\frac{1}{r}}} \quad \text{when } \sigma < f_u \qquad (1)$$

where $X = \varepsilon / \varepsilon_y$, $\varepsilon_y = f_y/E$ and $b = E_h/E$. The Von Mises yield criterion was used for representing the multiaxial stress state of steel.

2.4.2 Concrete

In contrast with the identical behaviour of steel in tension and compression, concrete presents a different mechanical response under compressive and tensile loads. Moreover, its mechanical behaviour is non-linear from the beginning of the deformation process. In stub columns subjected to compression, concrete expands laterally and the steel tubes provide a passive confinement, which may increase the strength and stiffness of concrete. In turn, in slender columns, the investigations carried out by Portoles *et al*. (2011a), Hassanein *et al*. (2015) and An *et al*. (2012) indicate that a certain passive confinement of concrete occurs due to the presence of the steel tube, increasing its ductility but not its strength.

Several concrete uniaxial models exist in the literature, which propose an enhancement in the compressive strength due to confinement, such as those from Zhao *et al*. (2002); Han and Huo (2003), Liang and Fragomeni (2009), Hu and Su (2011) or Pagoulatou *et al*. (2014). Nevertheless, in slender CFST columns, the increase in concrete strength by confinement is not significant (Portoles *et al*. 2011a). In effect, if the structural member is slender and the second

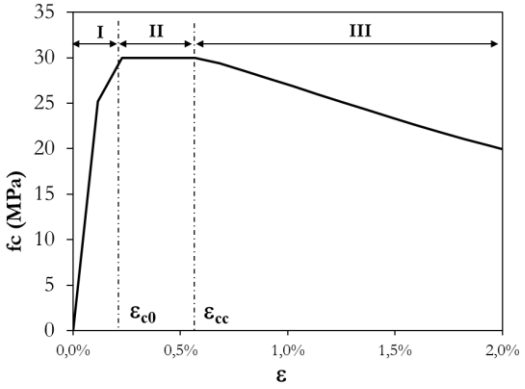

(a) NSC

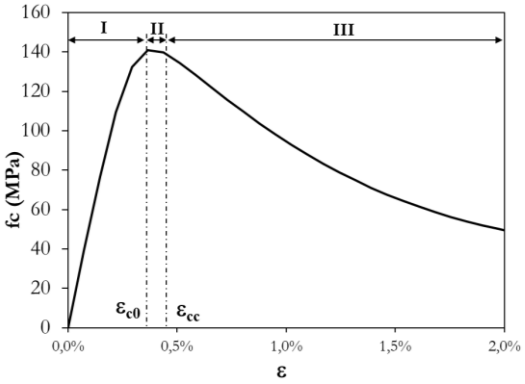

(b) UHSC

Fig. 5 Uniaxial model by Tao *et al*. (2013)

order effects are significant, the eccentricity of the axial force at the critical section is so large that the confinement effect on the concrete is insignificant, as concluded by Hajjar and Gourley (1996) and Liang (2009). In this sense, the models proposed by Hajjar and Gourley (1996), Han *et al*. (2007), Tao *et al*. (2013) were used, where the increase in compresive strength caused by confinement was not accounted for.

From the three aforementioned models, the model from Tao (Tao *et al*. 2013) was the one which provided a higher precision, according to the results of a previous sensitivity analysis (Pons Aliaga 2016), for both NSC and UHSC. The constitutive concrete model has a significant influence in the structural response of CFDST columns under compression, mainly in the peak load and post-peak branch. In Tao *et al*. (2013), these equations were experimentally validated for circular and square CFST stub columns infilled with USHC.

The model by Tao can be divided into three stages (Fig. 5(a)-(b)). In the ascending branch (I), there is not much interaction between the steel tube and concrete, thus a stress-strain relation without confinement is considered appropriate up to the compressive strength (f_c). Subsequently, a horizontal plateau (II) occurs up to the maximum strain by confinement (ε_{cc}). After reaching this point, the softening branch (III) initiates, where the increase in ductility caused by confinement is represented.

The first two stages of the model are governed by the proposal by Samani and Attard (2012). The ascencing brach is given by (2)

$$\frac{\sigma}{f_c} = \frac{AX + BX^2}{1+(A-2)X+(B+1)X}, \text{ when } 0<\varepsilon<\varepsilon_{c0} \quad (2)$$

where: $X = \varepsilon / \varepsilon_{cc}$;

$$A = \frac{\varepsilon_{co}}{f_c} E_c;$$

$$B = \frac{(A-1)^2}{0.55} - 1;$$

$$\varepsilon_{co} = 0.00076 + \sqrt{(0.626 f_c - 4.33)x10^{-7}}$$

f_c is the compressive cylinder strength (MPa); E_c is the estimated elastic modulus (MPa), obtained from the empirical expression provided by ACI 318 (ACI 2011), which expression is $E_c = 4.700 \cdot (f_c)^{0,5}$.

The second stage, horizontal, valid for circular columns, may be obtained by means of Eq. (3)

$$\varepsilon_{cc} / \varepsilon_{co} = e^k;$$
$$k = (2.9224 - 0.00367 f_c)(f_B / f_c)^{0.3124+0.002 f_c} \quad (3)$$

where: $f_B = \frac{(1+0.027 f_y)e^{0.002(D/t)}}{1+1.6e^{-10}(f_c)^{4.8}}$;

f_y is the steel yield strength (MPa);
D is the diameter of the steel tube (mm);
t is the steel tube wall thickness (mm).

Finally, the third stage (softening branch), is obtained through an exponential function proposed by Binici (2005), which formulation is

$$\sigma = f_r + (f_c - f_r)e^{-(\frac{\varepsilon-\varepsilon_{cc}}{\alpha})^\beta}, \text{ when } \varepsilon \geq \varepsilon_{cc} \quad (4)$$

where

$$f_r = -e^{-1.38\zeta} \quad f_c$$

when $f_r \leq 0.25 f_c$

$\alpha = 0.04 - 0.036 / (1 + e^{6.08\zeta - 3.49})$;

$\beta = 1.2$ (for circular section) and ζ is the confinement factor.

The confinement factor was developed for circular columns by Tao *et al*. (2004), with the following expression (5)

$$\zeta = (f_y / f_c)((D/(D-2t))^2 - 1) \quad (5)$$

It is worth noting that in the original formulation of the model from Tao *et al*. (2004), the authors used the expression for estimating the elastic modulus of concrete given by ACI 318 (ACI 2011), which does not especify the applicability range of f_c. In this work, the empirical formula given by Eurocode 2 Part 1.1 was used instead (CEN 2004a), where $E_c = 22000 \cdot (0.1 \cdot f_c)^{0.3}$, being f_c the compressive cylinder strength of concrete in MPa. The same modelling parameters have been used for all the

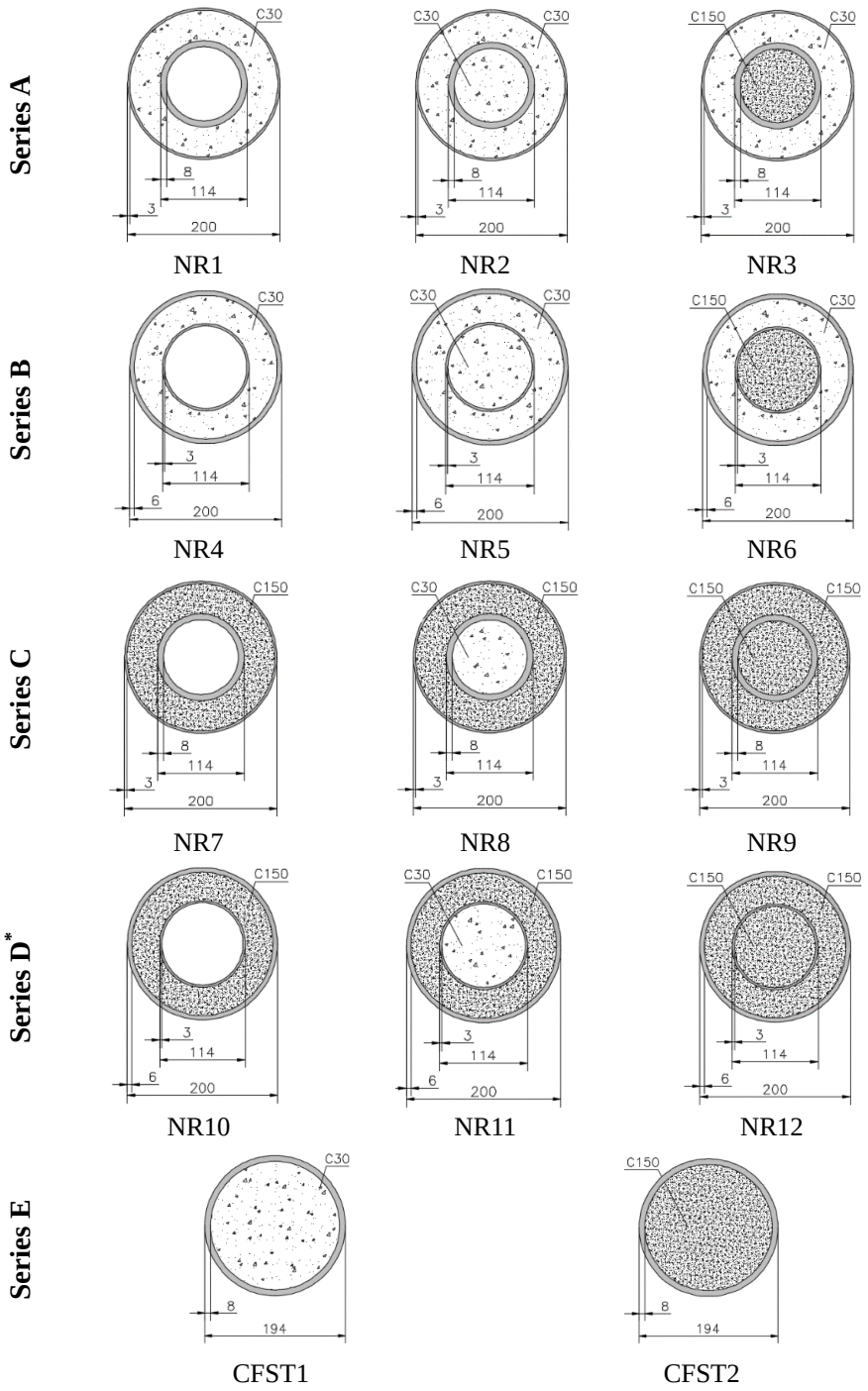

Fig. 6 Sectional dimensions of the CFDST and CFST columns from the experimental program (Romero *et al*. 2017)

concrete grades studied.

The Drucker-Prager yield criterion was used for representing the inelastic behaviour of concrete. This plasticity model is characterized by an associated flow rule and isotropic hardening, for which the dilation angle (ψ), friction angle (β) and the ratio of the yield stress in triaxial tension to the yield stress in triaxial compression (K) are needed. The values of these parameters were obtained from Hu and Su (2011) (ψ = 15°, β = 25°, K = 0.8), producing satisfactory results.

2.5 Contact between interacting surfaces

The mechanical interaction between contacting surfaces was defined in the model. A hard contact formulation was used for the normal interaction, while the tangent behaviour was modelled by means of a Coulomb friction model, with a friction coefficient of 0.25. This value has been used in a great number of numerical investigations on circular composite columns by other authors, as those presented by Hu and Su (2011); Hassanein *et al*. (2013); Tao *et al*. (2013) or Pagoulatou *et al*. (2014).

2.6 Analysis process

With the aim of obtaining a realistic response of slender CFDST columns under compressive load, it was necessary to carry out a nonlinear analysis, accounting for both geometric and material nonlinearities.

As starting geometry, the deformed shape corresponding to the initial imperfection of the column was introduced into the model. This initial imperfection depends on the manufacturing process and takes into account the out-of-straightness of the steel tubes. Several values of the initial imperfection can be found in the literature. In this case, a value of L/1000 was used, as recommended by Han *et al*. (2009) or Galambos and Surovek (2008).

A previous eigenvalue analysis of a hinged column under concentric axial load was carried out for obtaining the deformed shape corresponding to the first buckling mode. A unitary load was applied to the top end of the column, and the deformed shape was afterwards amplified by the imperfection factor L/1000. Subsequently, the deformed shape of the column was imported into the model as the starting geometry for conducting the mechanical analysis. Using the defined material properties, loads, boundary conditions and interactions, a nonlinear analysis was then carried out.

With all the exposed above, a realistic numerical model was developed, which allows simulating the mechanical behaviour of slender CFDST columns under concentric axial load. The computational cost of the simulations is judged reasonable, providing accurate results as will be proved in the next section.

3. Validation

3.1 Description of the experimental program

As described in the literature review, limited experimental work has been carried out to date on slender double-tube columns filled with normal strength concrete (NSC), and when it comes to CFDST columns using HSC, only the experiments from the authors of this paper can be cited. As this numerical work aims to investigate the behaviour of slender CFDST with different types of concrete filling –NSC and UHSC–, the test results from the previous experimental campaigns carried out by the authors (Romero *et al*. 2017) will be used for validation. In the referred experimental campaign, parameters such as the compressive strength of concrete, the distribution of concrete within the double tube cross-section and the inner and outer steel tube wall thickness were varied.

The experimental program consisted of 14 columns, 12 of which were CFDST columns and two of them were conventional CFST columns with a single steel tube, subjected to concentric axial load. More details on the test

Table 1 Mechanical properties of the materials used in the column tests*

	Id.	Code (CD_o-t_o-f_{co}_CD_i-t_i-f_{ci})	Outer steel tube			Concrete ring		Inner steel tube			Concrete core		ω
			f_{yo}	f_{uo}	E_{so}	f_{co}	E_{co}	f_{yi}	f_{ui}	E_{si}	f_{ci}	E_{ci}	
Series A	NR1	C200-3-30_C114-8-00	300	440	209358	36	32308	377	470	210002	--	--	2.25
	NR2	C200-3-30_C114-8-30	332	437	210510	45	34545	403	483	206939	42	33837	1.43
	NR3	C200-3-30_C114-8-150	272	436	203243	43	34077	414	500	217302	134	47924	0.87
Series B	NR4	C200-6-30_C114-3-00	407	471	180930	35	32036	343	445	209740	--	--	3.02
	NR5	C200-6-30_C114-3-30	377	462	190671	44	34313	329	426	210134	40	33346	1.51
	NR6	C200-6-30_C114-3-150	386	465	195988	43	34077	343	440	209169	123	46708	0.94
Series C	NR7	C200-3-150_C114-8-00	300	440	209358	138	48454	377	470	210002	--	--	0.59
	NR8	C200-3-150_C114-8-30	332	437	210510	139	48454	403	483	206939	43	34077	0.56
	NR9	C200-3-150_C114-8-150	272	436	203243	142	48765	414	500	217302	140	48662	0.42
Series D	NR10	C200-6-150_C114-3-00	407	471	180930	137	48244	343	445	209740	--	--	0.77
	NR11	C200-6-150_C114-3-30	377	462	190671	137	48244	329	426	210134	45	34545	0.61
	NR12	C200-6-150_C114-3-150	386	465	195988	146	49173	343	440	209169	140	48558	0.46
Series E	CFST1	C194-8-30	444	522	195623	40	33346	--	--	--	--	--	2.09
	CFST2	C194-8-150	444	522	195623	142	48454	--	--	--	--	--	0.59

* all the values in MPa

$\omega = (A_{yo} \times f_{yo} + A_{yi} \times f_{yi}) / (A_{co} \times f_{co} + A_{ci} \times f_{ci})$;
A_{yo} = outer steel tube area;
f_{yo} = yield strength of the outer steel tube;
f_{uo} = ultimate strength of the outer steel tube;
E_{so} = elastic modulus of the outer steel tube;
A_{yi} = inner steel tube area;
f_{yi} = yield strength of the inner steel tube;
f_{ui} = ultimate strength of the inner steel tube;

Table 2 Comparison between experimental and numerical ultimate load

	Id	Code	$\bar{\lambda}$	N_{EXP}	N_{NUM}	ξ_{E-N}
				(kN)		
Series A	NR1	C200-3-30_C114-8-00	0.74	1418	1404	1.01
	NR2	C200-3-30_C114-8-30	0.83	1627	1708	0.95
	NR3	C200-3-30_C114-8-150	0.87	1774	1767	1.00
Series B	NR4	C200-6-30_C114-3-00	0.72	1644	1586	1.04
	NR5	C200-6-30_C114-3-30	0.76	1964	1862	1.05
	NR6	C200-6-30_C114-3-150	0.85	2076	2122	0.98
Series C	NR7	C200-3-150_C114-8-00	0.96	2571	2481	1.04
	NR8	C200-3-150_C114-8-30	1.01	2862	2653	1.08
	NR9	C200-3-150_C114-8-150	1.05	3077	2791	1.10
Series D	NR10	C200-6-150_C114-3-00	0.90	2612	2586	1.01
	NR11	C200-6-150_C114-3-30	0.91	2793	2732	1.02
	NR12	C200-6-150_C114-3-150	1.01	3093	3084	1.00
				Mean		1.02
				Standard deviation		0.04

setup, instrumentation and test results can be found in Romero *et al*. (2017). The tested columns had a length (L) of 3315 mm and were hinged at both ends. The concrete used was NSC (f_c = 30 MPa) and UHSC (f_c = 150 MPa). Two steel grades were used, S275 and S355, depending on the steel tube wall thickness, as recommended by CEN (2006a, b).

The sectional dimensions were chosen so that the total steel area of the two steel tubes in the CFDST columns was equal to that of the outer steel tube in the reference CFST column (±4%). The tested sections are shown in Fig. 6. The experimentally obtained mechanical properties for the steel tubes and concrete are summarized in Table 1. These values were obtained from the uniaxial tensile tests performed over the steel coupons and concrete cylinder compression tests.

3.2 Validation of the numerical model

With the aim of verifying the accuracy of the numerical simulations against the experimental results, the error index (ξ_{E-N}) is defined (6). Expression (6) measures the error between the experimental (NEXP) and numerical (NNUM) ultimate load.

$$\xi_{E-N} = \frac{N_{EXP}}{N_{NUM}} \tag{6}$$

The previous expression provides information on the accuracy of the numerical simulations. Values greater than one mean safe predictions, while values lower than one represent unsafe predictions. Table 2 shows the values obtained for the analysed CFDST columns.

Through the developed numerical model, the nonlinear analysis of the 12 CFDST columns (series A to D) was carried out. The experimentally measured values of the material properties were used in the numerical simulations.

As can be seen in Table 2, safe predictions were obtained, with an average error of 1.02 and standard deviation equal to 0.04. Fig. 7 compares the experimental and numerical results. As can be seen, all the values are comprised within a ±10% interval, which evidences that the numerical model has a narrow dispersion and provides accurate predictions.

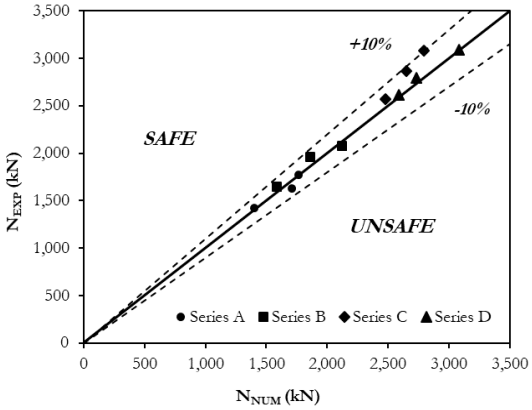

Fig. 7 Comparison between numerical and experimental results

Figs. 8 and 9 show the load-displacement curves for some of the columns analysed, where U1 is the transversal displacement at the mid-section of the column. A good agreement can be observed between the experimental and numerical curve, both in the peak load value and in the ascending and descending branches, what confirms the accuracy of the model.

4. Study on the mechanical performance of CFDST columns

Once the numerical model has been validated against the experimental results, it will be used in this section to perform a parametric study, in order to investigate the

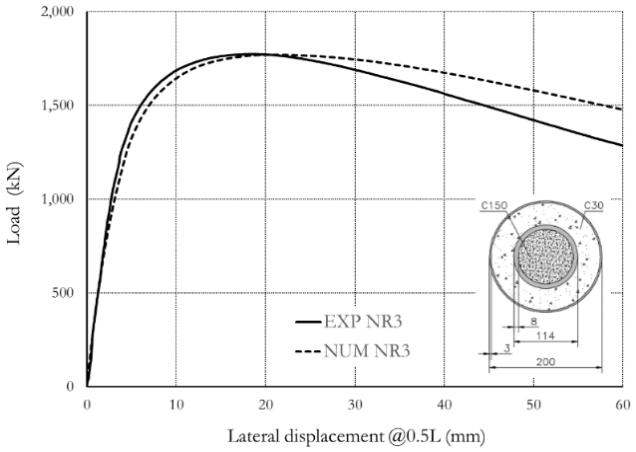

Fig. 8 Experimental versus numerical load-displacement curve, NR3 (C200-3-30_C114-8-150)

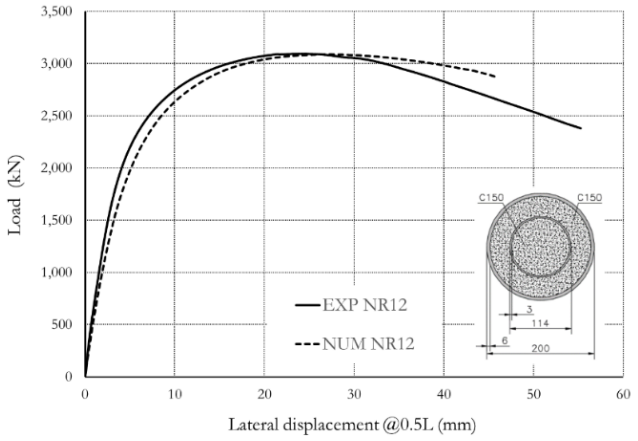

Fig. 9 Experimental versus numerical load-displacement curve, NR12 (C200-6-150_C114-3-150)

influence of the following parameters over the mechanical performance of CFST columns: non-dimensional slenderness ($\bar{\lambda}$), concrete strength – outer ring (f_{co}) and inner core (f_{ci}) – and the relation between the thicknesses of the inner and outer steel tubes (t_i/t_o). Based on the results of this parametric study, design recommendations will be given.

Apart from the maximum axial load of the column (N_{max}), other three strength indexes will be defined, with the aim of clarifying some practical aspects. For instance, these indexes will highlight to what extent does the load-bering capacity of CFDST columns improve that of conventional CFST columns. It will be also investigated in what situations is it appropriate to use UHSC, what is the best distribution of concrete within the double-tube cross-section or what is the best combination of thicknesses of the inner and outer steel tubes. The defined indexes may help evaluate the performance of CFDST columns, being the following: the *Strength Index* (SI), the *Concrete-Steel Contribution Ratio* (CSCR) and the *Inner Concrete Contribution Ratio* (ICCR).

4.1 Analysis cases

Table 3 presents the range of variation of the parameters studied, which were selected so as to accomplish with EN1994-1-1 (CEN 2004b), except for the upper limit of the concrete compressive strength, which can reach 150 MPa in this investigation. Nevertheless, this will help assess the validity of the current design methods for UHSC. A total number of 163 numerical simulations were carried out, combining all the parameters in Table 3. From the 163 analysis cases, 144 were CFDST columns and 19 were conventional CFST columns.

Table 3 Range of variation of the parameters in the parametric study

MEMBER PARAMETERS							
Non-dimensional slenderness	$\bar{\lambda}$	0.2	0.5	0.75	1	1.5	2
MATERIAL PARAMETERS							
Outer concrete strength	f_{co}(MPa)		--	30	90	150	
Inner concrete strength	f_{ci} (MPa)		0	30	90	150	
CROSS-SECTIONAL PARAMETERS							
Id	Dimensions (mm)						
	D_o		t_o		D_i		t_i
C3 (CFST)	198		4		--		--
C3_t-T (CFDST)	208		3.5		118		7.0
C3_T-t (CFDST)	208		6.0		118		2.5

* D_o = diameter of the outer steel tube;
t_o = wall thickness of the outer steel tube;
D_i = diameter of the inner steel tube;
t_i = wall thickness of the inner steel tube.

Using as a reference a conventional CFST section of dimensions 198 × 4 mm (C3), different CFDST sections were generated, with the criteria of maintaining the same total steel area in the cross-section. The reference column C3 was previously tested by Espinos *et al*. (2015) in an experimental campaing on CFST columns.

For the CFDST columns, the relation between thicknesses of the inner and outer steel tube was forced to be different from one, in order to generate two families of specimens: thin-thick (C3_t-T) or thick-thin (C3_T-t), where the first word refers to the outer steel tube and the second word refers to the inner steel tube. It is worth noting that the steel tube wall thicknesses were selected so as to avoid class 4 sections – i.e., local instabilities were prevented –.

In all the numerical simulations from this parametric study, the same characteristics of the numerical model described in Section 2 were used, except for the values of the mechanical properties of the materials which, in this case, were nominal values obtained from the European standards (CEN 2004a, b, 2005).

4.2 Analysis of results

4.2.1 Ultimate load (N_{max})

Fig. 10 represents the ultimate load (N_{max}) obtained from the parametric analysis for the range of slenderness studied (from 0.2 to 2). The influence of the wall thickness distribution in the section is studied, as well as the concrete

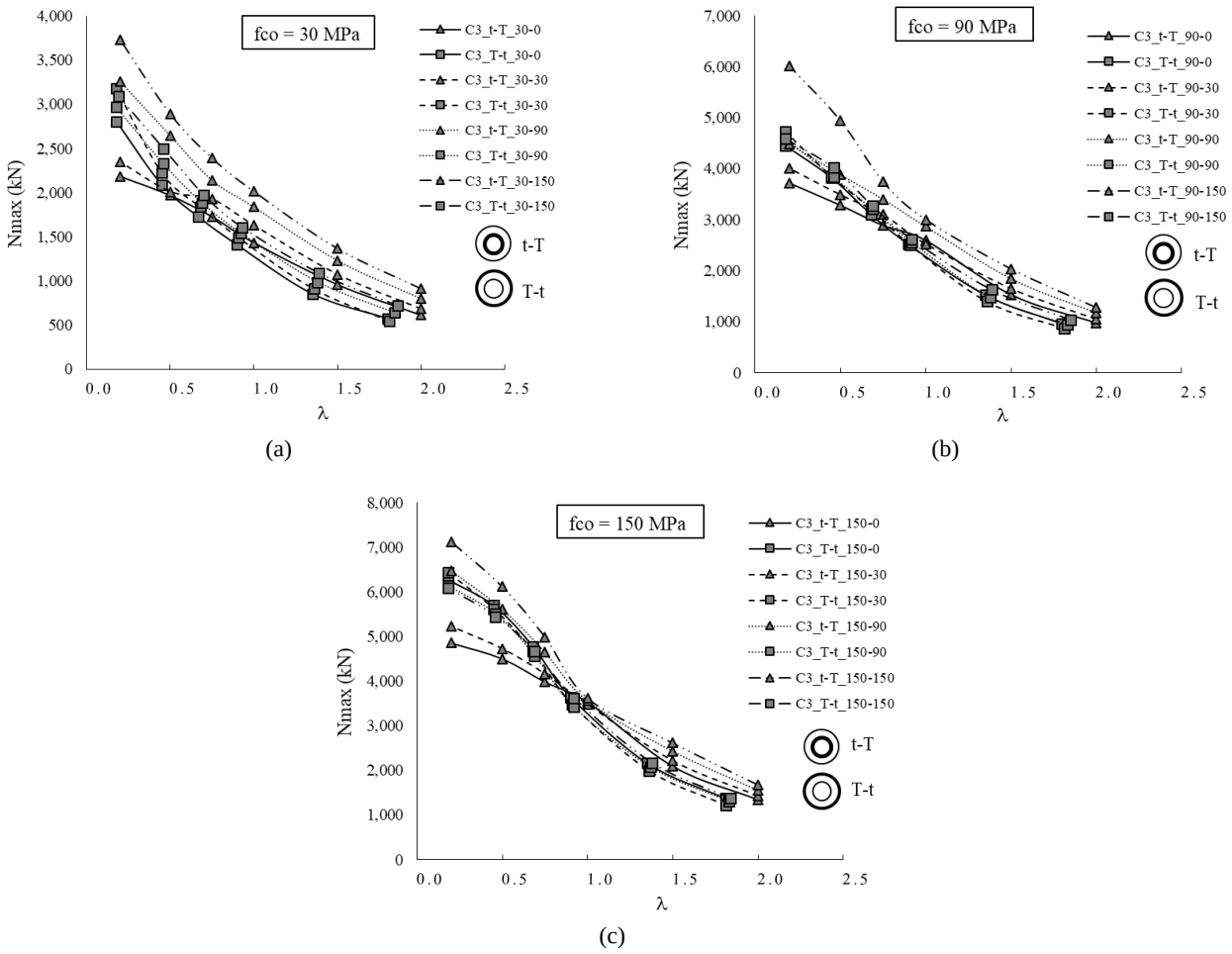

Fig. 10 Evolution of the ultimate load with the column slenderness, for different groups of concrete in the outer ring: (a) f_{co} = 30 MPa; (b) f_{co} = 90 MPa; (c) f_{co} = 150 MPa

strength. The results have been separated by series of outer ring concrete strength (f_{co} = 30, 90, 150 MPa), and for each series, the different inner core concrete strengths (f_{ci}) have been represented. In each graph, the groups C3_t-T and C3_T-t have been distinguished by different symbols (triangle for t-T, square for T-t). In the legend, C3_t-T_AA-BB, the last two letters stand for AA = f_{co}, BB = fc_i.

From the previous figures, it can be observed that the use of HSC or UHSC at the outer ring provides a significant increase of the load-bearing capacity of CFDST columns (compare values of N_{max} in Figs. 10(a), (b) and (c)). It can also be noticed in the three figures that for medium column slenderness (under 0.75 approximately), the distribution C3_t-T (thin-thick) results in lower values of N_{max} than the distribution C3_T-t (thick-thin) when the inner core is either unfilled or filled with NSC. In turn, if the inner core is filled with HSC (90 MPa) or UHSC (150 MPa), the distribution thin-thick (C3_t-T) provides a higher value of N_{max}. It is significant to note that after a certain slenderness, around 1, the distribution thin-thick (C3_t-T) results more convenient for all types of concrete filling. It is also worth noting that the inner concrete strength does not significantly influence the maximum capacity in the case of slender columns, when the outer concrete ring uses HSC or UHSC (see that the four lines in each group are close to each other).

4.2.2 Strength Index (SI)

The Strength Index (SI) is defined as the ratio between the ultimate load of the column (N_{max}) and the cross-sectional plastic resistance (N_{pl}) where, in this case, the increase in concrete strength due to confinement is neglected. This parameter provides direct information on the amount of reduction of the load bearing capacity of a column as compared to its cross-sectional plastic resistance, and can be understood as the buckling coefficient.

The cross-sectional plastic resistance is determined numerically from the results of N_{max} corresponding to the columns with relative slenderness $\bar{\lambda}$ = 0.2 ($N^{max}_{\bar{\lambda}=0.2}$) – i.e., stub columns –. Thus, the adapted expression for SI is as follows

$$SI = \frac{N^{max}}{N^{max}_{\bar{\lambda}=0.2}} \tag{7}$$

Fig. 11 plots the results of SI for the two families of columns analysed (C3_t-T and C3_T-t), together with the European buckling curves "a" and "b" from EN1993-1-1 (CEN 2005) and the theoretical Euler hyperbola.

It can be observed that in the range of slenderness (0.2 < λ < 1) most of the simulation results are comprised between the European buckling curves "a" and "b" (mostly the cases

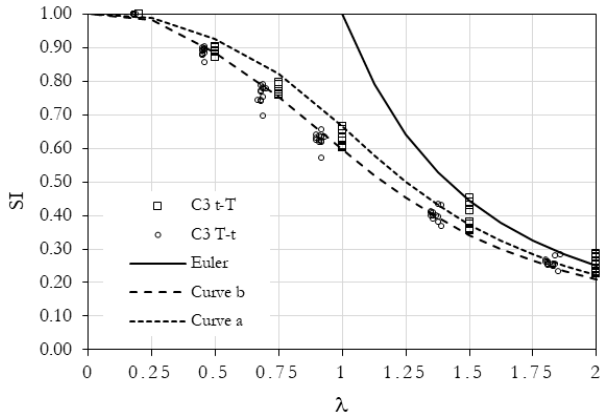

Fig. 11 Evolution of SI with the relative slenderness for the analysed columns

with thin-thick distribution) or even below buckling curve "a" for the cases of with thick-thin distribution. Nevertheless, for $\lambda > 1$ the results are mostly comprised between curves "a" and "b" or even above curve "b". This inversion in the general trend for slenderness values around 1 was already noticed when studying the ultimate load in Section 4.2.1. Therefore, it seems that the European buckling curves are conservative for values $\lambda > 1$, while for lower slenderness values their applicability to CFDST columns should be revised, as they may lead to unsafe results. It is also noteworthy that the values of the Strength Index for thin-thick distribution are generally higher than those for thick-thin distribution, and this happens for all the range of slenderness studied. This means that the second order effects are of less magnitude for these columns as compared with their sectional capacity.

4.2.3 Concrete-Steel Contribution Ratio (CSCR)

The index CSCR (Concrete-Steel Contribution Ratio) is a concept derived from the index CCR (Concrete Contribution Ratio), used in the literature for evaluating the performance of CFST columns as compared with hollow steel columns. In this case, CFDST columns contribute to increase the load bearing capacity of a conventional CFST column by means of both the concrete infill and the inner steel tube, increasing more significantly their performance.

The index CSCR is defined as the ratio between the ultimate load of the CFDST column ($N_{\mathrm{CFDST}}^{\max}$) and the ultimate load of an equivalent CFST column ($N_{\mathrm{CFST}}^{\max}$), which steel area is equal to the total steel area of the CFDST column (adding both inner and outer steel tube areas) and the concrete infill strength is equal to that of the outer ring of the CFDST column (f_{co}).

$$CSCR = \frac{N_{CFDST}^{\max}}{N_{CFST}^{\max}} \tag{8}$$

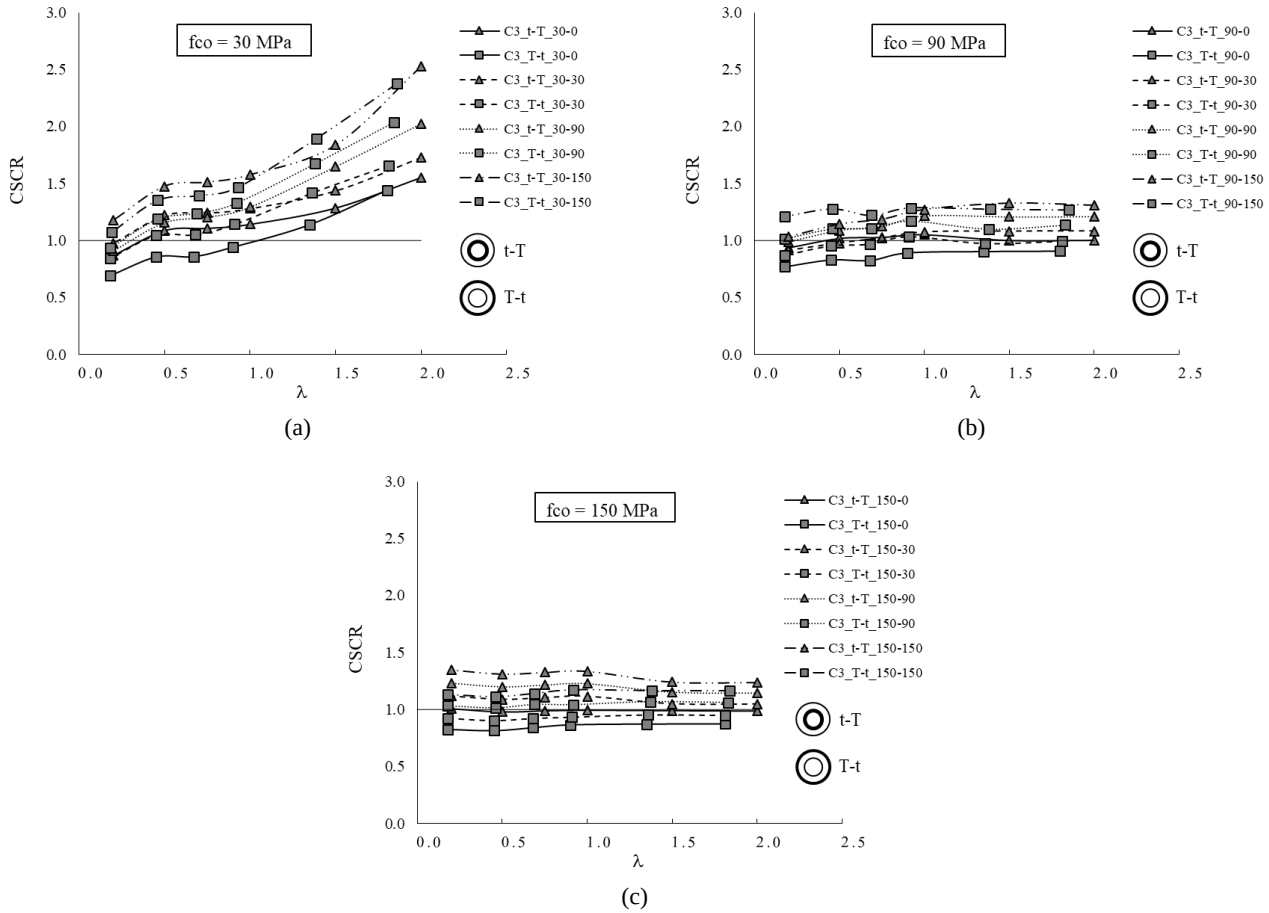

(a) (b)

(c)

Fig. 12 Evolution of the index CSCR with the column slenderness, for different groups of concrete in the outer ring: (a) f_{co} = 30 MPa; (b) f_{co} = 90 MPa; (c) f_{co} = 150 MPa

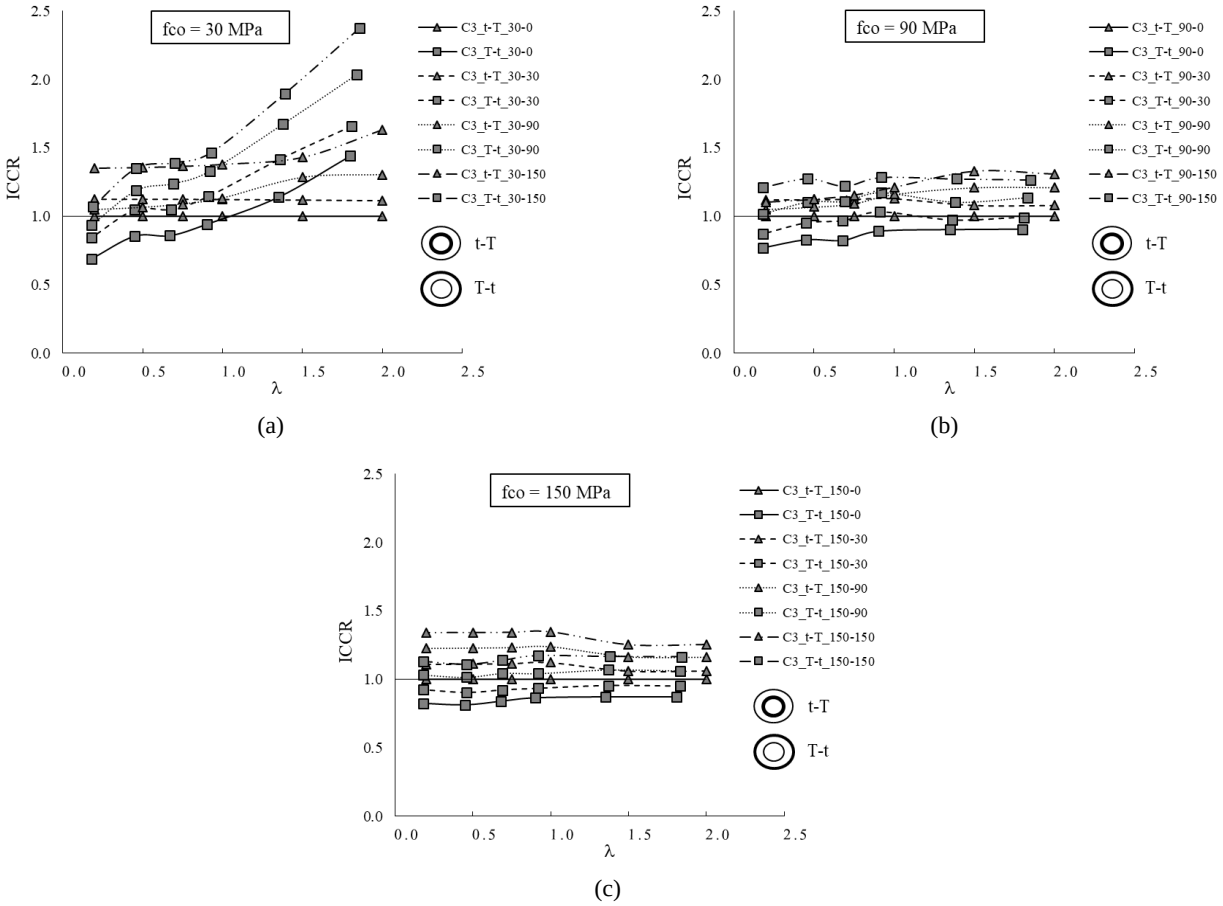

Fig. 13 Evolution of the index ICCR with the column slenderness, for different groups of concrete in the outer ring: (a) f_{co} = 30 MPa; (b) f_{co} = 90 MPa; (c) f_{co} = 150 MPa

According to this equation, when CSCR > 1, the double-tube column has a higher capacity than the CFST column, and thus an improvement of the mechanical performance is obtained through the addition of an inner tube. In turn, if CSCR < 1, the CFST column presents a higher load-bearing capacity that the double-tube column and therefore its use results inefficient.

Fig. 12 represents the values of the index CSCR obtained from the parametric analysis, for the range of slenderness studied (from 0.2 to 2). From this figure, it can be noticed the ascending trend of the index CSCR for the different families of columns when NSC is used in the outer ring (Fig. 11(a)), reaching values up to 2.5 for the combination f_{co} = 30 MPa, f_{ci} = 150 MPa. Nevertheless, this ascending trend cannot be appreciated when the concrete used at the outer ring is HSC or UHSC (Figs. 11(b), (c)), where the values of this index seem to stabilize around 1 - 1.25. What holds true for all groups of columns is that the CSCR index increases as the inner concrete strength is improved (see thinner lines above thicker lines in the three graphs). It is important to highlight that those columns without inner concrete infill (30-0, 90-0, 150-0) present values of CSCR close to one or even lower than one in some cases, meaning that they do not provide a significant enhancement of the column capacity as compared to the equivalent CFST column, or may even have an adverse effect. Regarding this matter, it should be pointed out that a double-skin column with CSCR ≈ 1 – i.e., with a similar capacity to that of the equivalent CFST column – makes use of a lower amount of concrete and therefore reduces the weight of the column. With regard to the distribution of thicknesses between the outer and inner tubes, it is not observed a significant influence over this coefficient, only being slightly higher the CSCR of the thin-thick distribution for the group with f_{co} = 150 MPa.

In Fig. 12(a), the concrete strength of the outer ring has been fixed (f_{co} = 30 MPa), and the trends for different inner concrete strength values are plotted (f_{ci} = 0-30-90-150 MPa). Those curves corresponding to HSC and UHSC present values of CSCR over one, for all the slenderness range. This means that HSC or UHSC as concrete infill provide a higher increase of the column capacity than NSC or using no concrete infill. The last type of columns (double-skin, i.e., 30-00) provides a certain grade of improvement for slenderness values over one. For values λ < 1, this option does not provide any increase of load-bearing capacity as compared to a conventional CFST column. Nevertheless, for λ > 1, the slope of the four curves increases, improving in all cases the CSCR index. Fig. 12(b) shows the curves corresponding to HSC at the outer ring (f_{co} = 90 MPa). Similarly to the previous case, those columns with HSC and UHSC as inner concrete infill provide values of CSCR > 1 and therefore improve the column capacity. When the concrete used at the outer ring is

UHSC, the relation changes significantly, as can be seen in Fig. 12(c). For $\lambda < 1$, the index CSCR may be considered independent of the slenderness. In turn, for $\lambda > 1$ the index ICSCR decreases as the slenderness increases. A certain improvement of the column capacity as compared to the reference CFST column is obtained in all the cases (CSCR ranging between 1 and 1.25), except for the curve corresponding to double-skin columns (150-00), which maintains the CSCR index close to one. In any case, not such important increase is obtained when using UHSC (similarly to HSC), as compared to the results previously obtained for NSC.

4.2.4 Inner Concrete Contribution Ratio (ICCR)

This parameter quantifies the improvement in the load-bearing capacity of CFDST columns when filling with concrete the inner steel tube, i.e., the enhancement that filling the inner tube (double-tube) provides to a double-skin column. It is defined as the ratio between the ultimate load of the double-tube column ($N^{\max}_{\text{CFDST ,double }-\text{tube}}$) and the ultimate load of the double-skin column ($N^{\max}_{\text{CFDST ,double }-\text{skin}}$) – i.e., the same column without concrete filling the inner steel tube –.

$$ICCR = \frac{N^{\max}_{CFDST,double-tube}}{N^{\max}_{CFDST,double-skin}} \tag{9}$$

To get a general view of the trend of the index ICCR, this parameter is plotted in Fig. 13 for different groups of f_{co}.

It can be seen how the values of ICCR generally decrease as the concrete at the outer ring increases its strength from NSC to UHSC. Inversely, the ICCR increases as the concrete strength at the inner core is improved, for a fixed value of f_{co}. Additionally, similar ratios between 1.1-1.3 are obtained when HSC or UHSC is used at the outer ring, while for the cases with NCS at the outer ring, higher differences are obtained for the different inner concrete grades.

It is important to note that for the cases with NSC at the outer ring (Fig. 13(a)), there is an influence of the slenderness on the index ICCR for thick-thin distribution, where ICCR increases for increasing slenderness, while for thin-thick distribution this influence is not so evident, remaining almost constant regardless the slenderness. This can be justified through the higher confinement index of the thick-thin distribution, what gives this section a superior mechanical performance.

In conclusion, it results convenient to fill the inner tube with concrete in those cases using NSC at the outer ring, while for cases with HSC or UHSC the benefit of filling the inner tube is marginal. Regarding the first case, the enhancement obtained through filling the inner core is much more significant for the thick-thin distribution and high slenderness values.

5. Conclusions

In this paper, the mechanical behaviour of CFDST columns subjected to concentric axial load has been investigated through a three-dimensional finite element model. The numerical model has been validated by comparison with experimental tests, showing satisfactory results. A parametric study has been subsequently performed for CFDST columns infilled with different grades of concrete: normal strength concrete (NSC), high strength concrete (HSC) and ultra-high strength concrete (UHSC). Two combinations of outer and inner steel tube wall thicknesses have been used (thin-thick and thick-thin). Through the results of this parametric study, it has been possible to obtain optimal combinations of the variables for an enhanced design of CFDST columns.

It has been observed that the use of HSC or UHSC at the outer ring provides a significant increase of the load-bearing capacity of CFDST columns. In turn, the use of these high performance concrete types at the inner core does not provide such an important benefit in terms of axial capacity. If the inner steel tube is unfilled or filled with NSC, the best combination of outer-inner tube thicknesses is thick-thin. In turn, if the inner steel tube is filled with HSC or UHSC, it is recommended to use the combination thin-thick for a better performance. The values of the Strength Index for thin-thick distribution have been found generally higher than those for thick-thin distribution, and this happens for all the range of slenderness studied, meaning that the second order effects are of less magnitude for these columns as compared with their sectional capacity. In general, it has been observed that the increase in strength of the inner concrete core provides higher values of the Strength Index. Through the index ICCR, it has been revealed that it is convenient to fill the inner tube with concrete in those cases using NSC at the outer ring, while for cases with HSC or UHSC at the outer ring, the benefit of filling the inner tube is marginal. Moreover, it has been found that the values of ICCR increase as the concrete strength at the inner core is improved, i.e., the contribution ratio improves when using HSC or UHSC.

These recommendations may be useful for an optimal design of CFDST columns, by selecting the adequate wall thicknesses of the inner and outer steel tubes and the appropriate combination of concrete grades filling the inner core and outer ring.

Acknowledgments

The authors would like to express their sincere gratitude to the "Conselleriad' Educació, Investigació, Cultura i Esport" of the Valencian Community (Spain) for the help provided through the project GV/2017/026.

References

ABAQUS (2014), ABAQUS/Standard Version 6.14 User's Manual: Volumes I-III, Pawtucket, Rhode Island, Hibbitt, Karlsson & Sorensen, Inc.

ACI (2011), Building code requirements for structural concrete (ACI 318-11), American Concrete Institute, Farmington Hills, MI, USA.

An, Y.-F., Han, L.-H. and Zhao, X.-L. (2012), "Behaviour and design calculations on very slender thin-walled CFST columns", *Thin-Wall. Struct.*, **53**, 161-175.

Binici, B. (2005), "An analytical model for stress–strain behavior of confined concrete", *Eng. Struct.*, **27**(7), 1040-1051.

CEN (2004a), EN 1992-1-1, Eurocode 2: Design of concrete structures. Part 1-1: General rules and rules for buildings; Comité Européen de Normalisation, Brussels, Belgium.

CEN (2004b), EN 1994-1-1, Eurocode 4: Design of composite steel and concrete structures. Part 1-1: General rules and rules for buildings; Comité Européen de Normalisation, Brussels, Belgium.

CEN (2005), EN 1993-1-1, Eurocode 3: Design steel structures. Part 1-1: General rules and rules for buildings; Comité Européen de Normalisation, Brussels, Belgium.

CEN (2006a), EN 10210-1: Hot finished structural hollow sections of non-alloy and fine grain steels - Part 1: Technical delivery conditions; ComitéEuropéen de Normalisation, Brussels, Belgium.

CEN (2006b), EN 10210-2: Hot finished structural hollow sections of non-alloy and fine grain steels - Part 2: Tolerances, dimensions and sectional properties; Comité Européen de Normalisation, Brussels, Belgium.

Chen, J., Ni, Y.-Y. and Jin, W.-L. (2015), "Column tests of dodecagonal section double skin concrete-filled steel tubes", *Thin-Wall. Struct.*, **88**, 28-40.

Elchalakani, M., Zhao, X.-L. and Grzebieta, R. (2002), "Tests on concrete filled double-skin (CHS outer and SHS inner) composite short columns under axial compression", *Thin-Wall. Struct.*, **40**(5), 415-441.

Espinos, A., Romero, M.L. and Hospitaler, A. (2010), "Advanced model for predicting the fire response of concrete filled tubular columns", *J. Constr. Steel Res.*, **66**(8-9), 1030-1046.

Espinos, A., Romero, M.L., Serra, E. and Hospitaler, A. (2015), "Circular and square slender concrete-filled tubular columns under large eccentricities and fire", *J. Constr. Steel Res.*, **110**, 90-100.

Essopjee, Y. and Dundu, M. (2015), "Performance of concrete-filled double-skin circular tubes in compression", *Compos. Struct.*, **133**, 1276-1283.

Galambos, T.V. and Surovek, A.E. (2008), *Structural Stability of Steel: Concepts and Applications for Structural Engineers*, Wiley.

Hajjar, J. and Gourley, B. (1996), "Representation of concrete-filled steel tube cross-section strength", *J. Struct. Eng.*, **122**(11), 1327-1336.

Han, L.H. and Huo, J.S. (2003), "Concrete-filled hollow structural steel columns after exposure to ISO-834 fire standard", *J. Struct. Eng.*, **129**, 68-78.

Han, L.-H., Yao, G.-H. and Tao, Z. (2007), "Performance of concrete-filled thin-walled steel tubes under pure torsion", *Thin-Wall. Struct.*, **45**(1), 24-36.

Han, L.-H., Huang, H. and Zhao, X.-L. (2009), "Analytical behaviour of concrete-filled double skin steel tubular (CFDST) beam-columns under cyclic loading", *Thin-Wall. Struct.*, **47**(6-7), 668-680.

Han, L.-H., Li, W. and Bjorhovde, R. (2014), "Developments and advanced applications of concrete-filled steel tubular (CFST) structures: Members", *J. Constr. Steel Res.*, **100**, 211-228.

Hassanein, M.F., Kharoob, O.F. and Liang, Q.Q. (2013), "Circular concrete-filled double skin tubular short columns with external stainless steel tubes under axial compression", *Thin-Wall. Struct.*, **73**, 252-263.

Hassanein, M.F., Kharoob, O.F. and Gardner, L. (2015), "Behaviour and design of square concrete-filled double skin tubular columns with inner circular tubes", *Eng. Struct.*, **100**, 410-424.

Hu, H.-T. and Su, F.-C. (2011), "Nonlinear analysis of short concrete-filled double skin tube columns subjected to axial compressive forces", *Marine Struct.*, **24**(4), 319-337.

Ibañez, C., Romero, M.L., Espinos, A., Portolés, J.M. and Albero, V. (2017), "Ultra-high Strength Concrete on Eccentrically Loaded Slender Circular Concrete-filled Dual Steel Columns", *Structures*, **12**, 64-74.

Liang, Q.Q. (2009), "Strength and ductility of high strength concrete-filled steel tubular beam–columns", *J. Constr. Steel Res.*, **65**(3), 687-698.

Liang, Q.Q. and Fragomeni, S. (2009), "Nonlinear analysis of circular concrete-filled steel tubular short columns under axial loading", *J. Constr. Steel Res.*, **65**(12), 2186-2196.

Menegotto, M. and Pinto, P.E. (1973), "Method of analysis for cyclically loaded R.C. plane frames including changes in geometry and non-elastic behaviour of elements under combined normal force and bending", *Proceedings of IABSE Symposium; Resistance and ultimate deformability of structures acted on by well defined repeated loads*, Lisbon, Portugal, **13**, pp. 15-22.

Pagoulatou, M., Sheehan, T., Dai, X.H. and Lam, D. (2014), "Finite element analysis on the capacity of circular concrete-filled double-skin steel tubular (CFDST) stub columns", *Eng. Struct.*, **72**, 102-112.

Pons Aliaga, D. (2016), "Estudio numérico de la capacidad portante de columnas mixtas con doble tubo rellenas de hormigón", Doctoral Thesis; Universitat Politècnica de València. [In Spanish]

Portoles, J.M., Romero, M.L., Bonet, J.L. and Filippou, F.C. (2011a), "Experimental study of high strength concrete-filled circular tubular columns under eccentric loading", *J. Constr. Steel Res.*, **67**(4), 623-633.

Portoles, J.M., Romero, M.L., Filippou, F.C. and Bonet, J.L. (2011b), "Simulation and design recommendations of eccentrically loaded slender concrete-filled tubular columns", *Eng. Struct.*, **33**(5), 1576-1593.

Romero, M.L., Espinos, A., Portolés, J.M., Hospitaler, A. and Ibañez, C. (2015), "Slender double-tube ultra-high strength concrete-filled tubular columns under ambient temperature and fire", *Eng. Struct.*, **99**, 536-545.

Romero, M.L., Ibañez, C., Espinos, A., Portolés, J.M. and Hospitaler, A. (2017), "Influence of ultra-high strength concrete on circular concrete-filled dual steel columns", *Structures*, **9**, 13-20.

Samani, A.K. and Attard, M.M. (2012), "A stress–strain model for uniaxial and confined concrete under compression", *Eng. Struct.*, **41**, 335-349.

Tao, Z., Han, L.H. and Zhao, X.L. (2004), "Behaviour of concrete-filled double skin (CHS inner and CHS outer) steel tubular stub columns and beam-columns", *J. Constr. Steel Res.*, **60**(8), 1129-1158.

Tao, Z., Wang, Z.-B. and Yu, Q. (2013), "Finite element modelling of concrete-filled steel stub columns under axial compression", *J. Constr. Steel Res.*, **89**, 121-131.

Zhao, X.L. and Han, L.H. (2006), "Double skin composite construction", *Progress in Structural Engineering and Materials*, **8**(3), 93-102.

Zhao, X.L., Grzebieta, R.H. and Elchalakani, M. (2002), "Tests of concrete-filled double skin CHS composite stub columns", *Steel Compos. Struct., Int. J.*, **2**(2), 129-142.

DL